ROLLING BEARING FAULT DIAGNOSIS BASED ON BRB AND PSO-SVM

Zhenghui LI[1*], Na ZHANG[2]

A rolling bearing fault diagnosis method based on belief-rule-base (BRB) and the particle swarm optimization (PSO)-based support vector machine (SVM) was proposed to solve the insufficient adjustment accuracy and long computation time due to the linear decrease of inertia weights cannot truly reflect the actual search process. Firstly, the ensemble empirical mode decomposition (EEMD) method was utilized to process the vibration information data of rolling bearing and decompose the information data into several intrinsic mode functions (IMFs), and then the root mean square of the IMFs was feature vector. The inference structure of BRB was built to obtain the estimates of inertia weight increments and update the historical inertia weights. Based on this inertia weight, the velocity, position and other parameters of each particle in PSO algorithm were adjusted and iterated sequentially until the stopping criteria were satisfied, then the optimization of PSO-SVM model parameters was realized. The datasets collected from two different experimental platforms in different environments were used to experiment with this method and other methods. This method contributes a novel attempt of effective adaptive adjustment of inertia weights in the existing method.

Keywords: Rolling bearing; Belief-rule-base; Inertia weight; Fault diagnosis

1. Introduction

Rotating machinery, as a very important power device, is widely used in industries such as mechanical engineering, water treatment, mining and quarrying[1-4]. The frequency of faults and accidents in rolling bearings is increasing due to the frequent exposure to heavy mechanical pressure and prolonged operation. According to statistics, the majority of faults in large mechanical power equipment are caused by bearing faults or damages[5-6]. The complexity of today's rotating machinery is increasing, and establishing an intelligent fault diagnosis system is the main direction of fault diagnosis research[7]. The overall process of fault diagnosis mainly consists of the following parts: (1) analyzing and processing of fault signal data; (2)selection and extraction of fault features in fault signal; (3)classification of fault type [8-9].

[1*] Prof., Electrical Engineering, Zhengzhou Railway Vocational & Technical College, China, e-mail: 15858190140@163.com
[2] PhD, Electrical Engineering, Zhengzhou Railway Vocational & Technical College, China, e-mail: zhangna@zzrvtc.edu.cn

Due to the high noise working environment of rotating machinery equipment, the obtained fault vibration signal data often contains noise and exhibits nonlinear characteristics. The commonly used methods for analyzing and processing fault signal data are Fourier transform (FT) and wavelet transform (WT)[10-11]. FT is a frequency domain analysis method for the entire signal, which cannot determine the time corresponding to the frequency. WT is an improved version of Fourier transform. It not only can complete analyzing and processing of fault signal data in the time domain, but can also can complete analyzing and processing of fault signal data in the frequency domain. But its adaptability in selecting wavelet functions is poor. The method for selecting and extracting fault features in fault signals is Empirical Mode Decomposition (EMD). Song et al.[12] used this method to analyze fault signals and converted them into images for fault diagnosis, achieving good experimental results. The adaptive data processing method decomposes any type of signal into several Intrinsic Mode Functions (IMFs), each representing local features of the original signal at different time scales. Relevant IMFs can be selected for signal analysis or recombination. However, EMD method suffer from pattern aliasing issues[13]. The Ensemble Empirical Mode Decomposition (EEMD) technique effectively addresses the pattern aliasing problems associated with EMD. It has better overall performance than EMD in analyzing vibration information[14-15].

The methods for classifying fault types and degrees include artificial neural networks (ANN), decision trees (DT), and support vector machines (SVM)[16-18]. Cavallaro et al.[16] optimized many parameters of ANN and provided some help and guidance for using this method. However, ANN based bearing fault diagnosis not only requires a sufficient number of samples, but also has a slow learning speed. The disadvantage of DT is the potential introduction of deviations. SVM can effectively solve the over-fitting and local optima issues of ANN.It has strong data mining and learning capabilities. In recent years, SVM has become a focus of international scholars in the field of fault diagnosis[17].

However, the fault diagnosis performance of SVM largely depends on a few parameters. Numerous experts and scholars have employed the Particle Swarm Optimization (PSO) algorithm to optimize the selection of crucial parameters in SVM, thereby enhancing its performance. And this attempt has been proven to achieve good results[18]. However, the process of finding the optimal important parameter values in PSO is nonlinear, but the inertia parameter weights are set to a linearly decreasing method, which cannot truly reflect the real particle search process. Based on a thorough analysis of existing inertia weight adjustment methods, this article tends to seek a method that can integrate and amplify the advantages of these methods while avoiding their disadvantages. The belief-rule-base (BRB) method proposed by Emam [19-20] can attempt to solve

these difficulties of insufficient adjustment accuracy and long computation time in the above methods, and achieve adaptive adjustment of inertia weights.

To overcome these difficulties, the article proposes a new method to solve the insufficient adjustment accuracy and long computation time due to the linear decrease of inertia weights cannot truly reflect the actual search process. Firstly, the EEMD method is utilized to process the vibration information data of rolling bearings and decompose the information data into several IMFs, and then the root mean square of the IMFs is feature vector. On the basis of the traditional PSO optimization model, an improvement plan is proposed to overcome premature convergence, low search accuracy and long computation time caused by improper selection of particle inertia weights. BRB is established to infer the estimated value of the change in inertia weight through belief rule inference, and update the inertia weight to achieve adaptive adjustment of inertia weight. Subsequently, based on the updated particle inertia weights, the velocity, position, global optimal value, and individual optimal value of each particle are adjusted. Based on this inertia weight, the velocity, position and other parameters of each particle in PSO algorithm are adjusted and iterated sequentially until the stopping criteria are satisfied, then the optimization of PSO-SVM model parameters is realized.

The remainder of this paper is organized as follows: Section 2 introduces the fundamental theory of fault signal processing and feature extraction in rolling bearings. Section 3 shows the construction process and operational steps of the proposed fault diagnosis method. Section 4 demonstrates the effectiveness of the proposed method through two experimental examples and provides a comparative analysis with other methods. Finally, Section 5 presents the conclusions.

2. Fault signal processing and feature extraction

2.1 Fault signal processing

(1) Firstly, the value of noise amplitude is determined based on the actual operating conditions, and the number of noise sets are set to M.

(2) In general, fault signal under actual operating conditions contains a lot of noise, while the original signal obtained through experiments contain less noise. In order to simulate actual operating conditions more realistically, a new fault signal is obtained by adding white noise data $n_i(t)$ to the original signal data $x(t)$.

$$x_i(t) = x(t) + n_i(t), i = 1,2,...,m \tag{1}$$

The i-th white noise is represented by $n_i(t)$. $x_i(t)$ represents the i-th new fault signal. t represents the time in the signal data.

(3) The new fault signal is further decomposed into IMF component by the EEMD algorithm.

$$x_i(t) = \sum_{x=1}^{S} c_{i,s}(t) + r_{i,s}(t) \tag{2}$$

S is the number of IMF components. The final residual, denoted as $r_{i,s}(t)$, represents the average trend of the signal. $c_{i,s}(t)$ is defined as IMF $(c_{i,1}, c_{i,2}, ..., c_{i,s}, ..., c_s)$, which represents the component information of signals in different frequency bands from high to low.

(4) Repeat step (2) M times with different white noise sequences to obtain a set of IMFs.

$$[\{c_{1,s}(t)\}, \{c_{2,s}(t)\}, ..., \{c_{M,s}(t)\}], s = 1,2,...,S \tag{3}$$

(5) Calculate the average value of the corresponding IMF sets and obtain the following result:

$$c_s(t) = \frac{1}{M}\sum_{i=1}^{M} c_{i,s}(t), i = 1,2,...,M; s = 1,2,...,S \tag{4}$$

$c_s(t)$ is the IMF component of EEMD decomposition.

2.2 Feature extraction

The feature extraction based on EEMD bearing fault diagnosis mainly relies on different fault locations and vibration signals generated by different fault degrees. Therefore, by extracting the features of vibration signals, different faults can be classified more accurately.

The commonly selected features for bearing fault diagnosis include kurtosis, margin, variance, root mean square, skewness, energy, etc. Reference [13] used many feature combinations, while this article only uses a single feature.

The root mean square value of bearing vibration signals mostly has a good correlation with the waveform of irregular vibrations generated by bearing surface wear. Therefore, this article summarizes and selects the test results of different features through testing in Table 1. Here, the results of two additional methods are presented for summary and comparison: the cuckoo search algorithm optimization support vector machine(CS-SVM) and the genetic algorithm optimization support vector machine(GA-SVM).

Table 1

Test of different features

Feature	CS-SVM/(%)	PSO-SVM/(%)	GA-SVM/(%)
Kurtosis	87.727 3	87.727 3	79.545 5
Mean value	59.545 5	58.181 8	54.090 9
Variance	91.727 3	91.454 5	79.090 9
Skewness	72.272 7	71.818 2	67.272 7
Root mean square	94.5786	95.636 4	87.272 8

Table 1 shows that the identification accuracy is highest when selecting root mean square features. Therefore, this article extracts the index of IMF as a feature for fault diagnosis. X_{rms} is the root mean square of IMF.

$$X_{rms} = \sqrt{\frac{\sum_{i=1}^{N} x_i^2}{N}} \tag{5}$$

The *i*-th sample value is represented by x_i. The number of samples is represented by *N*.

3. Fault feature classification

3.1 Theoretical derivation process of SVM

The fault classification process of SVM mainly involves constructing a suitable hyperplane equation $h(x)$ (Eq.6) to distinguish different types of samples. The training sample data is defined as $D=\{(x_1, y_1), (x_2, y_2)... (x_n, y_n)\}$, which contains several support vectors. A loss function $\varphi(w, \xi)$ is designed to improve the classification effect of the constructed hyperplane equation. When the value of the loss function is minimized, solve *w* and *b* using Eq.(7).

$$h(x) = w^T x + b \tag{6}$$

$$\min \varphi(w,\xi) = \frac{\|w\|^2}{2} + \frac{1}{2} C \sum_i^q \xi_i$$
$$s.t. y_i[g(x) - 1] \geq 0, \forall_i = 1,2,3,...,q \tag{7}$$

where *w* is a matrix, *b* and *C* are fixed parameters. The number of support vectors is defined as *q*. And the relaxation factor of each data point is represented as $\xi_i (\xi_i > 0)$.

The solving equation for Eq.(7) is defined as:

$$h(x) = \sum_{i=1}^{q} a_i \times y_i \times K(x, x_i) + b \tag{8}$$

Due to the high computational complexity of dot product operation in the feature vector space during the process of solving this equation, a kernel function $K(x, x_i)$ is designed to solve this problem. a_i is a Lagrange multiplier.

3.2 Inertial weight estimation of PSO based on BRB

This section specifically explains the process of inertia weight estimation based on BRB. The following content will provide a detailed introduction to BRB modeling and inference process from three aspects: BRB construction, BRB inference, and BRB integration.

3.2.1 BRB construction

(1) Determine the antecedent attribute and its reference value

In the BRB model for particle inertia weight estimation, the inertia weight w_i^h of particle p_i and the current performance evaluation index J_i^h at iteration times h are used as input feature variables f_1 and f_2, respectively. The change in inertia weight is used as the output of the model. The reference value set corresponding to input $f_m(m=1,2)$ is $A_m=\{A_{m,i}|i=1,2,...,K_m\}$, and the reference value set corresponding to the output feature variable is $D=\{D_n|n=1,2,...,N\}$, $A_{m,1}<A_{m,2}<....<A_{m,Km}$,$D_1<D_2<...<D_N$. K_m represents the number of reference levels for the m-th input feature variable, and N represents the number of reference levels for the output feature variable.

(2) Construct belief rule base

Based on the antecedent attribute and its reference value determined in Step1, and combined with expert experience, construct a belief rule base containing L rules. The l-th rule R_l is defined as:

$$R_1\text{:IF } (f_1 \text{ is } A_1^l) \text{ and } (f_2 \text{ is } A_2^l) \text{ THEN } \{(D_1,\beta_{1,l}),(D_2,\beta_{2,l}),\ldots,(D_N,\beta_{N,l})\} \quad (9)$$

$A_m^l(m=1,2;l=1,...,L)$ represents the reference level of the m-th antecedent attribute in rule l, and satisfies $A_m^l \in A_m=\{A_{m,\theta}\,|\,\theta=1,2,...,K_m\}$; $\beta_{n,l}(n=1,...,N)$ represents the belief level assigned to the reference level in rule l.

3.2.2 BRB inference

(3) Calculate matching degree

For the obtained input feature vector $X(h,i)=[f_1(h,i),f_2(h,i)]$, input $f_m(h,i)$ can be converted into the form of a reliability distribution, and the corresponding weight $X(h,i)$ can be calculated:

$$w_l=\frac{\theta_l\prod_{m=1}^{2}(\alpha_m^l)^{\bar{\delta}_m}}{\sum_{l=1}^{L}\left[\theta_l\prod_{m=1}^{2}(\alpha_m^l)^{\bar{\delta}_m}\right]} \quad (10)$$

Here, activate weight $w_l\in[0,1]$, $\bar{\delta}_m$ is relative attribute weight, a_m^l is the matching level between the input $f_m(h,i)$ and its reference value under rule l.

3.2.3 BRB integration

(4) Rule combination

After obtaining the corresponding weights of the rules, the activation rules with corresponding weights are fused using ER. The belief level of the output reference value corresponding to the input feature vector $X(h, i)$ can be calculated:

$$\hat{\beta}_n=\frac{u\left[\prod_{l=1}^{L}(w_l\beta_{n,l}+1-w_l\sum_{n=1}^{N}\beta_{n,l})-\prod_{l=1}^{L}(1-w_l\sum_{N=1}^{N}\beta_{n,l})\right]}{1-u[\prod_{l=1}^{L}(1-w_l)]} \quad (11)$$

$$u = \left[\sum_{n=1}^{N} \prod_{l=1}^{L} (w_l \beta_{j,l} + 1 - w_l \sum_{n=1}^{N} \beta_{n,l}) - (N-1) \prod_{l=1}^{L} \left(1 - w_k \sum_{l=1}^{L} \beta_{n,l} \right) \right]^{-1} \tag{12}$$

$$O(X(h,i)) = \{(D_n, \hat{\beta}_n), n = 1, 2, \mathrm{L}\ , N\} \tag{13}$$

(5)Estimate particle inertia weight

Calculate the change in inertia weight $\Delta w(h,i)$ based on the rule fusion results obtained in Step 4. The inertia weight w_{i+1}^h of particle p_{i+1} is calculated at the h-th iteration process:

$$\Delta w(h,i) = \sum_{n+1}^{N} D_n \hat{\beta}_n \tag{14}$$

$$w_{i+1}^h = w_i^h + \Delta w(h,i) \tag{15}$$

At this point, the estimation of the inertia weight of particle p_{i+1} in the h-th iteration process has been completed.

3.3 The overall process flow of fault diagnosis

An improved plan is proposed based on the traditional PSO model to address issues of premature convergence, low search accuracy, and extended computation time, which arise from the improper selection of particle inertia weights. BRB is established to infer the estimated value of the change in inertia weight through belief rule inference, and update the inertia weight to achieve adaptive adjustment of inertia weight. Subsequently, based on the updated particle inertia weights, the velocity, position, global optimal value, and individual optimal value of each particle are adjusted. Based on this inertia weight, the velocity, position and other parameters of each particle in PSO algorithm are adjusted and iterated sequentially until the stopping criteria are satisfied, then the optimization of PSO-SVM model parameters is realized. Specifically, input the actual data x into the model to obtain the output y_o. The fitness value of particles is calculated based on model error. The optimal solution is determined based on fitness values and stopping criteria. Figure 1 shows a detailed flowchart.

The flowchart reveals that the processing primarily comprises three components: (1) the detailed process of EEMD and SVM; (2) the optimization process of PSO; and (3) the updated model of inertia weight based on BRB.

(1)The detailed process of EEMD and SVM. The process is primarily divided into three stages: analyzing and processing fault signal data, selecting and extracting fault features, and classifying fault types. Initially, the acquired sample datasets serve as input data for the model. The EEMD method is employed to decompose the sample data signals and calculate the IMFs. Subsequently, the calculated and extracted sample datasets are input into the SVM model for training and testing.

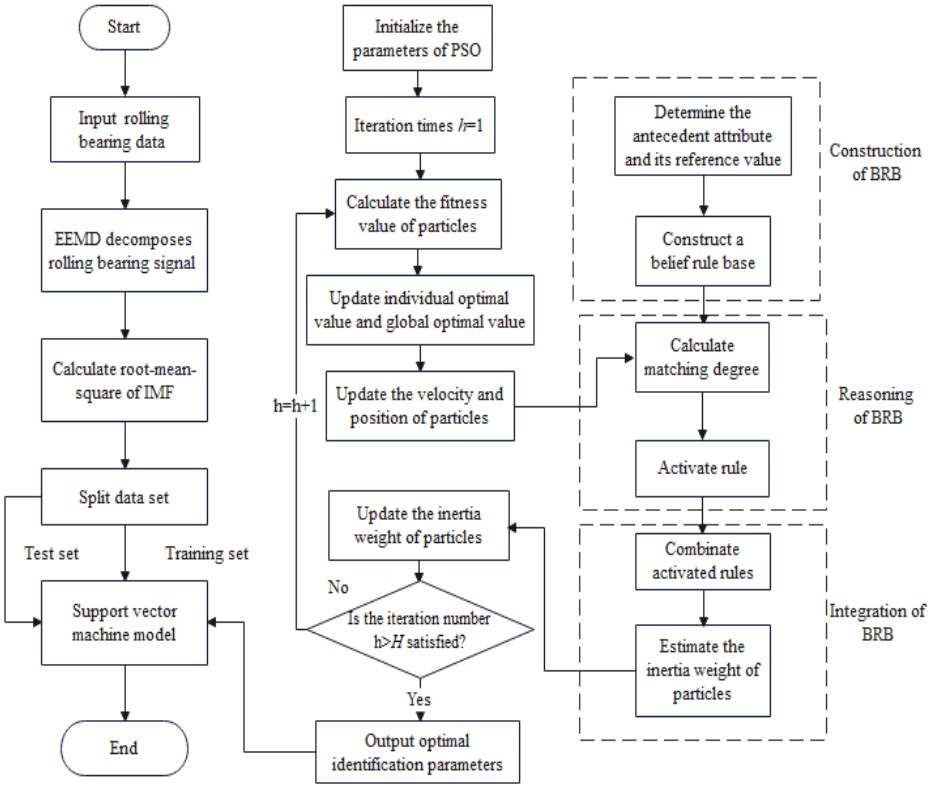

Fig. 1. The flowchart of the proposed method

(2)The optimization process of PSO. This process is mainly divided into: the initialization of the model,calculate the fitness value of particles and update the inertia weight of particles. Firstly, the PSO parameters are initialized based on empirical values. Secondly, the fitness of the particle swarm is calculated, and both the individual optimal value and the global optimal value are updated. The vectors and positions of the particle swarm are then updated using the designed BRB. If either the number of iterations or the accuracy meets the specified requirements, the loop process terminates. Otherwise, if both the number of iterations and accuracy do not meet the requirements, the loop continues to iterate and train. Finally, the output of the optimal identification parameters is utilized to optimize the SVM model.

(3)The update model of inertia weight based on BRB. The linear decrease of inertia weights in PSO cannot adequately reflect the search process required to find the optimal solution. This process comprises three main stages: construction of the BRB, reasoning within the BRB, and integration of the BRB. Initially, the antecedent attributes and their reference values are determined through expert knowledge, and the BRB is constructed using multiple belief rules. The vectors and positions of the particles are then input into this belief rule base. Subsequently,

several belief rules are matched to varying degrees and activated. The activated rules are calculated using an evidence reasoning fusion algorithm, and the inertia weights of the particles are subsequently updated based on the fusion results. This entire process functions as a nested loop.

4. Experiment and analysis

4.1 Experimental condition

The experimental environment and platform of the article are shown in the figure 2(Case Western Reserve University). The left side of the platform includes: fan and bearing,induction motor, drive and bearing. The central section of the platform consists of a coupling and a torque transducer/encoder. The right section of the platform is a dynamometer. The control electronics are not shown in the figure.Electric discharge machining technology was used to simulate pitting faults on bearings from weak to severe. The data from the measuring points were collected by sensors positioned near the bearings, which were the diagnostic objects at the motor drive end and the fan end[21].

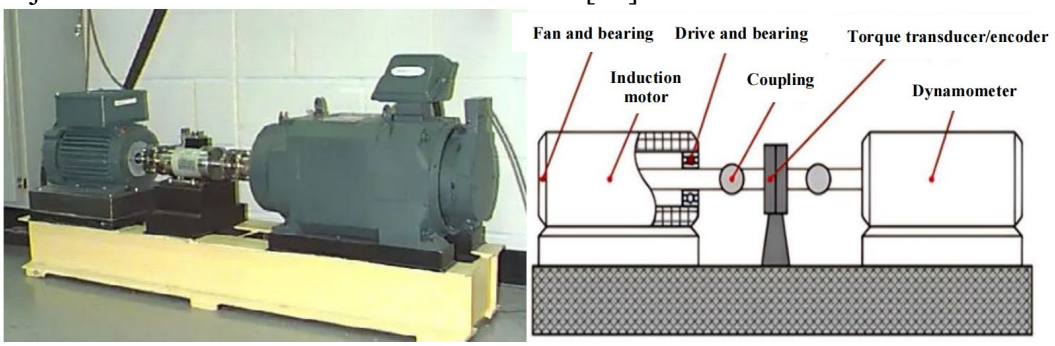

Fig. 2. The experimental environment and platform

This experiment collected a total of 10 types of sample data information, including normal data, inner ring fault (diameter 0.18mm, 0.36mm, 0.53mm,0.71mm), rolling element fault (diameter 0.18mm), outer ring fault 0.18mm (3-point position, 6-point position, 12 o'clock position), outer ring fault (diameter 0.36mm, 0.53mm).There are a total of 200 sets of sample data for each fault type. 104 sets are selected from these 200 sets to train the important parameters of the model, and the other data is used to test the accuracy of this model.

4.2 Results and analysis

This study uses the EEMD method for data processing and extracts the root mean square of 14 transformed IMFs (if less than 14, use 0 padding) as feature inputs.The three methods(BRB-PSO-SVM, PSO-SVM, GA-SVM) were iterated 100 times, 200 times, and 500 times respectively.The test comparison results of average fitness and average accuracy are shown in Table 2.

Table 2 shows that compared to PSO-SVM and GA-SVM, BRB-PSO-SVM has certain improvements in convergence speed and diagnostic accuracy. This is because PSO has fixed inertia weights during the search process, which makes it difficult to adjust the ability of global and local search well, resulting in lower identification performance than BRB-PSO. However, GA-SVM shows a linearly decreasing trend in inertia weight during the identification process. Although it improves the accuracy of identification to a certain extent, it cannot adapt well to nonlinear identification problems.

The belief rule in BRB-PSO is developed based on the traditional IF-THEN rule, and its output is a structure of belief distribution, which has the ability to model nonlinear uncertain input-output relationships. The input activated rules are fused and inferred by the Evidence Based Reasoning (ER) algorithm, which can obtain more refined parameter identification results.

Table 2

Test results of different algorithms

Methods	Iterations	Average fitness value	Average accuracy
PSO-SVM	100	0.7449	92.5
	200	0.8656	94.0
	500	0.3567	95.0
GA-SVM	100	0.9567	87.2
	200	0.9653	87.8
	500	0.9346	88.1
BRB-PSO-SVM	100	1.5673E-05	98.9
	200	1.5673E-05	99.9
	500	1.5673E-05	99.9

To verify the effectiveness of this method, 960 sets of test data are applied to the above three methods, and Figure 3-5 show the detailed comparative diagnostic results of the experimental data.The red solid line represents the actual fault type, while the blue dashed line illustrates the fault type diagnosis results obtained from the corresponding method.

(1)GA-SVM mistakenly diagnoses non-fault type as fault type, and misdiagnosis can also occur between faults of different severity levels on the inner ring, rolling elements at different fault positions, and faults of different severity levels on the outer ring.

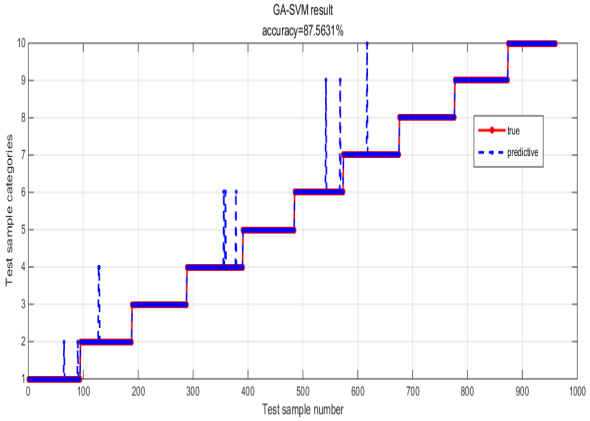

Fig. 3. Test accuracy of GA-SVM

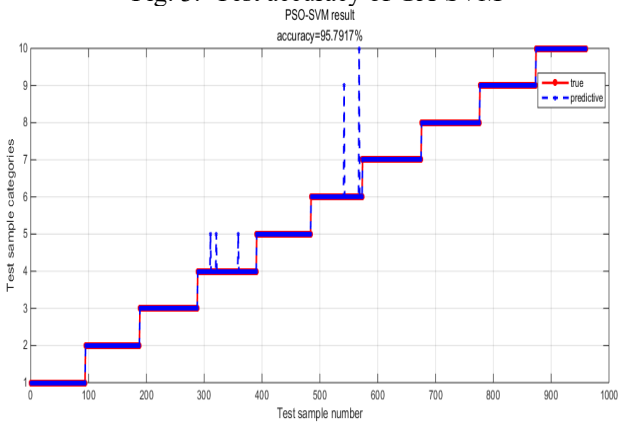

Fig. 4. Test accuracy of PSO-SVM

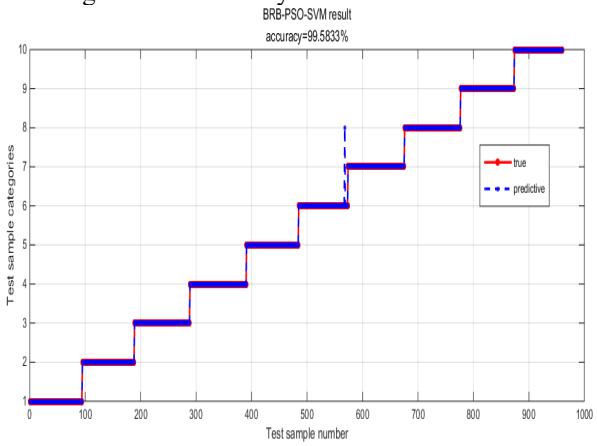

Fig. 5. Test accuracy of BRB-PSO-SVM

(2)PSO-SVM is very accurate in diagnosing non-fault type, faults at different positions of rolling elements, and faults of different severity levels on the outer ring, but it may lead to misdiagnosis between faults of different severity levels on the inner ring.

(3)BRB-PSO-SVM is highly accurate in diagnosing faults at different locations and severity levels.

This article adopted the method of taking the average of 50 experiments for result comparison. The comparison of different classification methods is shown in Table 3.

Table 3

Comparison of diagnostic accuracy and time consumption of different methods

Methods	Diagnostic accuracy(%)	50 times consumption(s)
PSO-SVM	95.5	16.2
GA-SVM	88.7	23.84
BRB-PSO-SVM	100	23.61

Experiments have shown that although the diagnostic time of BRB-PSO-SVM is not the shortest, it is within an acceptable range.Under the condition of not increasing the diagnostic time too much, the diagnostic accuracy of BRB-PSO-SVM is superior to traditional PSO-SVM and GA-SVM.

4.3 The other experimental platform and its result analysis

This study conducted experiments in other experimental environment and platform as shown in the figure 6 (Cincinnati University). On the left side of the figure is accelerometer, the middle part of the figure is radial load, and the right part of the figure is thermocouples. This data sets are divided into normal data, inner ring fault, outer ring fault, and rolling fault[22]. The results generated by the new experimental environment and platform are shown in Table 4.

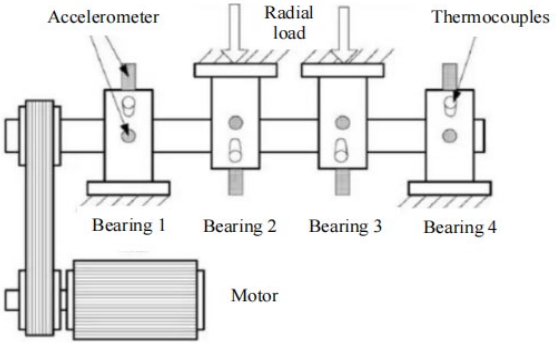

Fig. 6. The experimental platform structure

Table 4

Comparison of diagnostic accuracy and time consumption of different methods

Methods	Diagnostic accuracy(%)	50 times consumption(s)
PSO-SVM	96.5	18.21
GA-SVM	89.6	26.83
BRB-PSO-SVM	98.97	21.71

Experiments on bearing data from the Cincinnati University have shown that BRB-PSO-SVM performs better than PSO-SVM and GA-SVM on different data platforms.

5. Conclusion

This article uses the EEMD method to decompose signal data and extracts the root mean square of IMF components as features. On the basis of the traditional PSO optimization model, an improvement plan is proposed to overcome premature convergence, low search accuracy and long computation time caused by improper selection of particle inertia weights. BRB is established to infer the estimated value of the change in inertia weight through belief rule inference, and update the inertia weight to achieve adaptive adjustment of inertia weight. Subsequently, based on the updated particle inertia weights, the velocity, position, global optimal value, and individual optimal value of each particle are adjusted. The above process is iterated sequentially until the stopping condition is met, achieving optimization of the SVM model. Finally, data sets from different experimental environments and platforms are used for validation, which not only accurately identified the location of bearing faults, but also outperformed traditional PSO-SVM and GA-SVM in terms of accuracy.

This paper ends with the following future research ideas: (1)Future research will use detection data from real complex environments to further test the robustness of this method. Due to the differences in data distribution and fault features between detection data in real complex environments and detection data in experimental simulation environments, the future work will further improve the overall performance of this method based on these differences. (2)The proposed method is a meaningful attempt to overcome linear decrease of inertia weights cannot truly reflect the actual search process required to find the optimal solution. However, the unbalance of fault data will bring new challenges to this method. Therefore, the future work will attempt knowledge transfer and reinforcement learning methods to improve the cross domain adaptability of the model.

(3)This article is a attempt to use expert knowledge to guide data-driven fault diagnosis method. The next work will explore more ideas that combine knowledge and data to improve this field technology.

Acknowledgement

This work was financially supported by Key scientific research projects of colleges and universities in Henan Province (25A580011) and Scientific &Technological Research Project in Henan Province (242102240130).

REFERENCES

[1] *Muhammad N, Albezzawy, Mohamed G, et al.* Rolling element bearing fault identification using a novel three-step adaptive and automated filtration scheme based on Gini index, ISA Transactions, 101, 2020, pp.453-460.

[2] *Zhi Q Z, Yang B L, Guan Q Q, et al.* A review of the application of deep learning in intelligent fault diagnosis of rotating machinery, Measurement, 206, 2023, 112346.

[3] *El L.M, Wang L, Harvey T.J*, et al. Further understanding of rolling contact fatigue in rolling element bearings—A review. Tribology International, 140, 2019, 105849.

[4] *Liu J, Shao Y.* Overview of dynamic modelling and analysis of rolling element bearings with localized and distributed faults. Nonlinear Dyn, 93, 2020, pp. 1765–1798.

[5] *Miao Y, Zhang B, Li C*, et al. Feature Mode Decomposition: New Decomposition Theory for Rotating Machinery Fault Diagnosis. IEEE Transactions on Industrial Electronics, 70(2), 2023, pp. 1949-1960.

[6] *Zhu H, Xie C, Fei Y*, et al. Attention mechanisms in CNN-based single image super-resolution: A brief review and a new perspective. Electronics, 10(10), 2021, 1187.

[7] *Gao Z, Liu X.* An overview on fault diagnosis, prognosis and resilient control for wind turbine systems. Processes, 9(2), 2021, 300.

[8] *Leite V C*, et al. Detection of localized bearing faults in induction machines by spectral kurtosis and envelope analysis of stator current. IEEE Trans. Ind. Electron, 62(3),2015, pp. 1855-1865.

[9] *Abid A, Khan M.T,* et al. A review on fault detection and diagnosis techniques: basics and beyond. Artif Intell Rev, 54, 2021, pp. 3639–3664.

[10] *Huang S, Wang X, Li C*, et al. Data decomposition method combining permutation entropy and spectral substitution with ensemble empirical mode decomposition. Measurement, 139, 2019, pp.438–453.

[11] *Wang D, Zhao Y, Yi C*, et al. Sparsity guided empirical wavelet transform for fault diagnosis of rolling element bearings. Mech. Syst. Signal Process, 101,2018, pp. 292–308

[12] *Sun, Y.J, Li, S.H, Wang, X.H,* et al. Bearing fault diagnosis based on EMD and improved Chebyshev distance in SDP image. Measurement, 176, 2021,109100.

[13] *Ali D, Mir M, Reza H,* et al. A hybrid fine-tuned EMD and CNN scheme for untrained compound fault diagnosis of rotating machinery with unequal-severity faults. Expert Systems with Applications, 157, 2021,114094.

[14] *Yan X, Liu Y, Zhang W*, et al. Research on a novel improved adaptive variational mode decomposition method in rotor fault diagnosis. Applied Sciences, 10(5), 2020, 1696.

[15] *Sun S, Przystupa K, Wei M*, et al. Fast bearing fault diagnosis of rolling element using Levy Moth-Flame optimization algorithm and Naive Bayes. Maintenance and Reliability, 22, 2020, pp. 730–740.

[16] *Cavallaro L, Bagdasar O, De Meo. et al*. Artificial neural networks training acceleration through network science strategies. Soft Comput, 24, 2020, pp. 17787–17795.

[17] *Cuong Le T, Nghia T, Khatir S*. et al. An efficient approach for damage identification based on improved machine learning using PSO-SVM. Engineering with Computers, 38, 2022, pp. 3069–3084.

[18] *Mocanu D.C, Mocanu E, Stone P,*et al.Scalable training of artificial neural networks with adaptive sparse connectivity inspired by network science. Nat. Commun, 9 2018, 2383.

[19] *Emam H, Mohammad S. H, Pär-Ola Z*, et al. Machine learning with Belief Rule-Based Expert Systems to predict stock price movements. Expert Systems with Applications, 206, 2022,117706.

[20] *R. U. Islam, M. S. Hossain and K. Andersson*. A Deep Learning Inspired Belief Rule-Based Expert System. IEEE Access, 8, 2020, pp. 190637-190651.

[21] *Shen W, Xiao M, Wang Z,* et al. Rolling Bearing Fault Diagnosis Based on Support Vector Machine Optimized by Improved Grey Wolf Algorithm. Sensors, 23(14), 2023, 6645.

[22] *Zhong X, He L, Zhao X*. Bearing Fault Diagnosis Based on SVMD and Parameter Optimization MCKD. Journal of Mechanical & Electrical Engineering, 7(5), 2024, pp.1001-4551.